Received: 2 July 2020 | Revised: 25 September 2020 | Accepted: 19 October 2020

DOI: 10.1096/fj.202001668R

RESEARCH ARTICLE

THE FASEB JOURNAL

TNF-α signaling regulates RUNX1 function in endothelial cells

Hannah A. B. Whitmore[1,2] | **Dhanesh Amarnani**[1,2] | **Michael O'Hare**[1,2] | **Santiago Delgado-Tirado**[1,2] | **Lucia Gonzalez-Buendia**[1,2] | **Miranda An**[1,2] | **Julien Pedron**[3] | **John H. Bushweller**[3] | **Joseph F. Arboleda-Velasquez**[1,2] | **Leo A. Kim**[1,2]

[1]Schepens Eye Research Institute of Massachusetts Eye and Ear Infirmary, Boston, MA, USA

[2]Department of Ophthalmology, Harvard Medical School, Boston, MA, USA

[3]Department of Molecular Physiology and Biological Physics, University of Virginia, Charlottesville, VA, USA

Correspondence
Leo A. Kim, Schepens Eye Research Institute of Massachusetts Eye and Ear Infirmary, 20 Staniford Street, Boston, MA 02143, USA.
Email: leo_kim@meei.harvard.edu

Funding information
National Eye Institute of the National Institutes of Health, Grant/Award Number: R01EY027739; E. Matilda Zieger Foundation for the Blind; Karl Kirchgessner Foundation; Michel Plantevin; National Cancer Institute of the National Institutes of Health, Grant/Award Number: R01CA234478

Abstract

Runt-related transcription factor 1 (RUNX1) acts as a mediator of aberrant retinal angiogenesis and has been implicated in the progression of proliferative diabetic retinopathy (PDR). Patients with PDR, retinopathy of prematurity (ROP), and wet age-related macular degeneration (wet AMD) have been found to have elevated levels of Tumor Necrosis Factor-alpha (TNF-α) in the eye. In fibrovascular membranes (FVMs) taken from patients with PDR RUNX1 expression was increased in the vasculature, while in human retinal microvascular endothelial cells (HRMECs), TNF-α stimulation causes increased RUNX1 expression, which can be modulated by RUNX1 inhibitors. Using TNF-α pathway inhibitors, we determined that in HRMECs, TNF-α-induced RUNX1 expression occurs via JNK activation, while NF-κB and p38/MAPK inhibition did not affect RUNX1 expression. JNK inhibitors were also effective at stopping high D-glucose-stimulated RUNX1 expression. We further linked JNK to RUNX1 through Activator Protein 1 (AP-1) and investigated the JNK-AP-1-RUNX1 regulatory feedback loop, which can be modulated by VEGF. Additionally, stimulation with TNF-α and D-glucose had an additive effect on RUNX1 expression, which was downregulated by VEGF modulation. These data suggest that the downregulation of RUNX1 in conjunction with anti-VEGF agents may be important in future treatments for the management of diseases of pathologic ocular angiogenesis.

KEYWORDS
angiogenesis, endothelial cell, RUNX1, TNF-α, signaling pathway

Abbreviations: AMD, age-related macular degeneration; AP-1, activator protein 1; BCA, bicinchoninic acid assay; CNV, choroidal neovascularization; DR, diabetic retinopathy; ECs, endothelial cells; FVM, fibrovascular membrane; HPRT, hypoxanthine phosphoribosyltransferase 1; HRMECs, human retinal microvascular endothelial cells; JNK, c-Jun N-terminal kinases; LDH, lactate dehydrogenase (Cell death) assay; NF-κB, nuclear Factor kappa-light-chain-enhancer of activated B cells; PDR, proliferative diabetic retinopathy; RUNX1, runt-related transcription factor 1; ROP, retinopathy of prematurity; P38/MAPK, p38 mitogen-activated protein kinases; PRP, panretinal photocoagulation; TNF-α, tumor necrosis factor-alpha; TNFR1, tumor necrosis factor receptor 1; VEGF, vascular endothelial growth factor.

1 | INTRODUCTION

We,[1] and others[2] have previously identified the transcription factor Runt-related transcription factor 1 (RUNX1) in mediating aberrant retinal angiogenesis in patients with proliferative diabetic retinopathy (PDR). Aberrant ocular angiogenesis is a common pathologic mechanism, which causes a variety of blinding diseases of the eye including retinopathy of prematurity (ROP),[3] proliferative diabetic retinopathy (PDR), and exudative or wet age-related macular degeneration (wet AMD).[4,5] RUNX1 is the alpha-subunit, of a heterodimeric complex also comprising Core-binding factor β (CBFβ), which confers increased DNA binding and stability to the complex.[1] Transcriptome studies using patient-derived fibrovascular membranes from patients with PDR, demonstrated high RUNX1 expression within vascular endothelial cells (ECs). In vitro studies using human retinal microvascular endothelial cells (HRMECs) showed that RUNX1 regulates endothelial cell proliferation, migration, and tube formation, demonstrating a strong link between RUNX1 expression and vessel growth,[1] while in vivo work shows that RUNX1 inhibition using an inhibitor of RUNX1 driven transcription, Ro5-3335, shows preclinical efficacy in the oxygen-induced retinopathy model. The formation of abnormal blood vessels is thought to be primarily mediated by vascular endothelial growth factor (VEGF),[5-8] a master regulator of angiogenesis in development and disease. It is unclear how RUNX1 signaling intersects with VEGF, while the mechanism linking high glucose and inflammation to RUNX1 upregulation and aberrant angiogenesis is also poorly understood.

As Tumor Necrosis Factor-alpha (TNF-α) plays a key role in initiating pathologic angiogenesis in a variety of clinical conditions, we hypothesized that TNF-α may modulate RUNX1 expression in ECs and we investigated these cell signaling pathways to understand their role in mediating RUNX1 expression in ECs. TNF-α is a proinflammatory cytokine, originally thought to be only secreted by macrophages [9] although it can also be produced by endothelial cells.[10] There are conflicting roles of TNF-α reported, with it generally considered anti-angiogenic in vitro and pro-angiogenic in vivo.[11-13] TNF-α has been linked to insulin-resistance, obesity, cell apoptosis, and breakdown of the blood-retinal-barrier[14-16] and as such has been connected to several blinding eye diseases involving the retina. TNF-α is reported to be present at elevated levels in retinal diseases such as wet-AMD[17-19] and ROP,[20,21] where a high level within 3 days of birth is associated with an increase in severity. Although a consistently high blood glucose level is the most common hallmark of uncontrolled diabetes mellitus, TNF-α has also been implicated as a biomarker of PDR.[14,22] TNF-α is found in increased levels in the plasma, vitreous fluid, and tears of diabetic patients with PDR[14,23] but is not present in the retinal tissues of healthy individuals.[24-26] It has been detected in the fibrovascular membranes (FVMs) of PDR patients and plays an important role in PDR pathogenesis.[22] TNF-α receptor signaling is known to activate the NF-κB, p38/MAPK, and JNK pathways[27] most commonly through binding the receptors TNFR1 or TNFR2.

Anti-VEGF therapy has been found to be variably effective in the treatment of ROP,[3,28] PDR,[29] and wet AMD.[4] Anti-VEGF therapy has been shown to be effective in the treatment of PDR[8] when compared to panretinal photocoagulation (PRP).[30] However, both PRP and anti-VEGF therapy have been associated with worsening PDR with a cumulative risk of 42% and 34%, respectively, over two years.[31] The use of anti-VEGF therapy for wet AMD has been validated through multiple clinical trials,[32,33] yet the need for regular intravitreal injections, the potential risk of retinal atrophy with chronic anti-VEGF therapy,[4,34] and a subgroup of patients who are non-responders to anti-VEGF therapy[35] are all potential limitations of anti-VEGF therapy in the management of wet AMD. Hence, there is a need to identify targets beyond VEGF for the treatment of pathologic ocular angiogenesis.

2 | MATERIALS AND METHODS

Surgical samples for FVM analysis were collected at Massachusetts Eye and Ear (MEE). The Internal Review Board of MEE approved this study and all participants gave informed consent prior to surgery and inclusion in the study. The research protocols adhered to the Association for Research in Vision and Ophthalmology (ARVO) Statement on Human Subjects and the tenets of the Declaration of Helsinki.

The mouse model experimental protocol was reviewed and approved by the Institutional Animal Care and Use Committee (IACUC) of MEE. All animal procedures were performed in accordance with the ARVO Statement for the Use of Animals in Ophthalmic and Vision Research.

2.1 | Chemicals and reagents

Tumor Necrosis Factor-alpha (TNF-α), Transforming Growth Factor beta 1 (TGFβ1), Transforming Growth Factor beta 2 (TGFβ2) and Interleukin 6 (IL-6) were purchased from PeproTech (Rocky Hill, NJ, USA). Recombinant human VEGF 165 protein was purchased from R&D Systems (Minneapolis, MN, USA). Aflibercept (Eylea) was purchased from Regeneron Pharmaceuticals (Tarrytown, NY, USA). D-glucose, mannitol, L-glucose, and RUNX1 inhibitor Ro5-3335 were purchased from Millipore-Sigma (Burlington, MA, USA). Small-molecule inhibitors and activators purchased from commercial sources included TNF-α-TNFR1 binding inhibitor CAY10500 and JNK activator

anisomycin, (Santa Cruz Biotechnology, Dallas, TX, USA); NF-κB inhibitors Caffeic acid phenethyl ester (CAPE) and Honokiol; dual NF-κB and JNK inhibitor Withaferin A, JNK inhibitors SP600125 and TCS JNK 6o; p38/MAPK inhibitors SB259063 and SB202190 (Tocris Bioscience, Bristol, UK); and AP-1 inhibitor, SR11302 (R&D Systems). The CBFβ-RUNX1 protein–protein interaction inhibitor, AI-14-91, and an inactive control compound of similar chemical structure, AI-4-88, were synthesized as described previously.[36]

2.2 | Choroidal neovascularization model

Six to eight-week-old C57BL6/J mice (Jackson Laboratory, Bar Harbor, ME) were anesthetized with a Ketamine/Xylazine mixture. Four laser spots were performed around the optic nerve of one eye (120 mW, 50 ms, and a spot size of 50 μm). Postlaser injury, the mice were maintained under standard housing conditions and three days after laser induction, mice were euthanized and eyes collected for further analysis.

2.3 | Cell culture

Human retinal microvascular endothelial cells (HRMECs) purchased at P3 from Cell Systems Corporation (Kirkland, WA, USA) were incubated at 37°C with 5% CO_2. HRMECs were plated at P6 using endothelial growth media (EGM-2) (Lonza, Basel, Switzerland) supplemented with 2% FBS (Atlanta Biologicals, GA, USA), 1% penicillin/streptomycin, and 1% L-glutamine (Lonza). Cells were treated at P7 in endothelial basal media (EBM-2) (Lonza) supplemented with 2% FBS, 1% penicillin/streptomycin, and 1% L-glutamine and selected stimulants. Cell starvation media was EBM-2 alone.

2.4 | qRT-PCR analysis

Unless otherwise stated, cells for qRT-PCR analysis were treated for 48 hours before being lysed. RNA was extracted using RNeasy Mini Kits (QIAGEN, Hilden, Germany) as per the manufacturer's instructions. Transcription into complementary DNA was performed using the iScript cDNA synthesis kit (Bio-Rad, Hercules, CA, USA), following the manufacturers' protocol, and probed using FastStart Universal SYBR Green Master Mix (Hoffmann-La Roche, Basel, Switzerland) in 384-well white plates. Primers for selected genes (Table 1) were purchased from Integrated DNA Technologies (Coralville, IA, USA).

2.5 | Protein isolation and Western Blot analysis

Unless otherwise stated, cells for western blot analysis were treated for 72 hours before being lysed. Cells were lysed using RIPA buffer (Cell Signaling Technology, Danvers, MA, USA) and protein concentration measured using the bicinchoninic acid (BCA) assay kit (Thermo Fisher Scientific, Inc Waltham, MA, USA). A total of 10-20 μg of protein was separated by 4-20% Mini-PROTEAN TGX precast gels (Bio-Rad, Hercules, CA, USA) and transferred to Immobilon™-FL PVDF transfer membranes (Thermo Fisher Scientific, Inc). Membranes were dried overnight, wetted with methanol, and blocked with Odyssey Blocking Buffer (LI-COR Biosciences, Lincoln, NE, USA) for 1 hour prior to incubation with primary antibodies, mouse anti-RUNX1 (sc-365644), mouse anti-p-RUNX1 (sc-293146), mouse anti-JNK (sc-7345) mouse anti-p-JNK (sc-6254) (Santa Cruz Biotechnology) and rabbit anti-β-actin antibody (4970S, Cell Signaling Technology) for 4 hours at room temperature (RT). Membranes were subsequently washed with TBST and incubated with secondary antibodies (IRDye 680RD donkey anti-rabbit and IRDye 800CW donkey anti-mouse (dilution 1:4000) (LI-COR Biosciences). After rinsing twice with TBST, immunoreactive bands were visualized using the Odyssey Infrared Imaging System, and band intensities normalized to β-actin were quantified using Image Studio version 2.1 (LI-COR Biosciences).

2.6 | Immunohistochemistry

Human FVM membranes from PDR patients were fixed in 10% formalin (Millipore-Sigma) in Dulbecco's phosphate-buffered saline (PBS) (Millipore-Sigma) overnight at RT and stored in PBS at 4°C until paraffin embedding. Serial sections (6 μm) were cut, deparaffinized in 100% xylene, rehydrated in an ethanol-wash series, and washed in PBS. For heat-induced antigen retrieval, the slides were boiled in 10 mM sodium citrate buffer (pH 6.0) and then maintained at

TABLE 1 Primer sequences used in qRT-PCR analysis

Primer	Forward	Reverse
HPRT1 (housekeeping)	ACCCTTTCCAAATCCTCAGC	GTTATGGCGACCCGCAG
RUNX1	TCCACAAACCCACCGCAAGT	CGCTCGGAAAAGGACAAGC
JNK1	TCTGGTATGATCCTTCTGAAGCA	TCCTCCAAGTCCATAACTTCCTT

a sub-boiling temperature (95-100°C) for 20 minutes and subsequently cooled on the benchtop for 30 minutes. Slides were washed with distilled water and permeabilized with 0.5% Triton X-100 in PBS for 5 minutes and blocked (10% donkey serum in PBS) for 1 hour at RT. Samples were incubated with primary antibodies rabbit anti-human AML1/RUNX1 IHC-plus (LS-B13948, Lifespan Biosciences, Seattle, WA), and mouse anti-human TNFR1 antibody (sc-8436; Santa Cruz Biotechnology) overnight at 4°C. Membranes were washed with PBS and incubated with secondary antibodies, donkey anti-rabbit Alexa Fluor 647 (A-31573, Invitrogen, Carlsbad, CA, USA) and donkey anti-mouse Alexa Fluor 594 (A-21203, Invitrogen) for 2 hours at RT. Slides were mounted and visualized using Prolong Gold Antifade Reagent with DAPI (P36935, Invitrogen). Images were obtained using a Leica SP8 Confocal microscope (Leica microsystems, Wetzlar, Germany) at 63× magnification with oil immersion.

In vivo CNV mouse model flatmounts were permeabilized as above and blocked with 5% bovine serum for 30 minutes at RT. Flatmounts were incubated with primary antibodies (rabbit anti-human AML1/RUNX1 IHC-plus (LS-B13948) and mouse anti-human TNFR1 antibody (sc-8436)) as above. Flatmounts were washed with PBS and incubated with secondary antibodies (donkey anti-rabbit Alexa Fluor 647 (A-31573) and donkey anti-mouse Alexa Fluor 594 (A-21203)) as above. Flatmounts were mounted and visualized using Prolong Gold Antifade Reagent with DAPI (P36935, Invitrogen). Images were obtained using an Axio Imager M2 fluorescence microscope (Zeiss, Oberkochen, Germany) at 20× magnification.

2.7 | Immunocytochemistry

HRMECs were seeded into 48-well plates and treated in treatment media with selected conditions for 72 hours. Cells were washed once with PBS and fixed using 4% paraformaldehyde (PFA, Thermo Fisher Scientific, Inc). Cells were permeablized with Triton (0.01%), blocked with 5% goat serum, and incubated with primary antibodies, rabbit anti-human AML1/RUNX1 IHC-plus (LS-B13948, LifeSpan Biosciences), mouse anti-human CD31 (M082329, Agilent, Santa Clara, CA, USA), mouse anti-human TNFR1 (sc-8436, Santa Cruz Biotechnology) for 4 hours at room temperature. Cells were washed with PBS and incubated with secondary antibodies, goat anti-rabbit Alexa Fluor 594 (A11012, Invitrogen), goat anti-mouse Alexa Fluor 488 (A11001, Invitrogen), Hoechst 33 342 fluorescent nucleic acid stain (ImmunoChemistry Technologies, Bloomington, MN, USA) for 1 hour before imaging on an EVOS imaging system (Thermo Fisher Scientific, Inc).

To determine the nuclear localization of RUNX1, cells were cultured on glass cover slips in 6 well plates in treatment media with selected conditions for 72 hours. Cells were fixed, permeabilized, and blocked as above. Cells were incubated with primary antibody (rabbit anti-human AML1/RUNX1 IHC-plus (LS-B13948)) and secondary antibodies (goat anti-rabbit Alexa Fluor 594 (A11012) and Hoechst 33 342) as above. Following this, cells were incubated with conjugated Phalloidin, Alexa Fluor 488 (8878, Cell Signaling Technologies) for 15 minutes before cover slips were mounted using Prolong Gold Antifade Reagent (P36934, Invitrogen). Images were obtained using a Leica Sp8 Confocal microscope at 63× magnification with oil immersion.

2.8 | Cell proliferation assay

HRMECs were seeded into 96 well plates and treated in treatment media with selected conditions for 24 or 48 hours. Half the media volume was removed (100 µl) prior to proliferation analysis for future lactate dehydrogenase (LDH) assay. Cells were then incubated with the CyQUANT Direct Cell Proliferation Assay kit (C35011, Thermo Fisher Scientific, Inc) and the resulting fluorescence imaged as per the manufacturer's instructions. Cells for LDH Max and LDH assay media were stored overnight in the freezer (−80°C). Samples were defrosted and analyzed using the CytoTox96 Non-radioactive Cytotoxicity Assay (Promega, Madison, WI, USA) as per the manufacturer's instructions.

2.9 | Scratch-wound migration assay

Migration was assessed with the scratch-wound assay. HRMECs were treated for 24 hours. Treatment media was switched to EBM-2 starvation media for 8 hours. One scratch was generated per well and imaged on an EVOS imaging system for 12 hours. Images were analyzed using ImageJ.

2.10 | Statistical analysis

Results are graphed as mean ± SEM. Ordinary one-way ANOVA (Dunnett's correction) was used for comparisons between multiple groups. A P value $< .05$ was considered significant.

3 | RESULTS

3.1 | Co-localization of TNFR1 and RUNX1 in FVMs, CNV lesions, and HRMECs

We previously found increased RUNX1 expression within HRMECs and in ECs in FVMs derived from PDR patients.[1] To determine whether our previously reported findings of

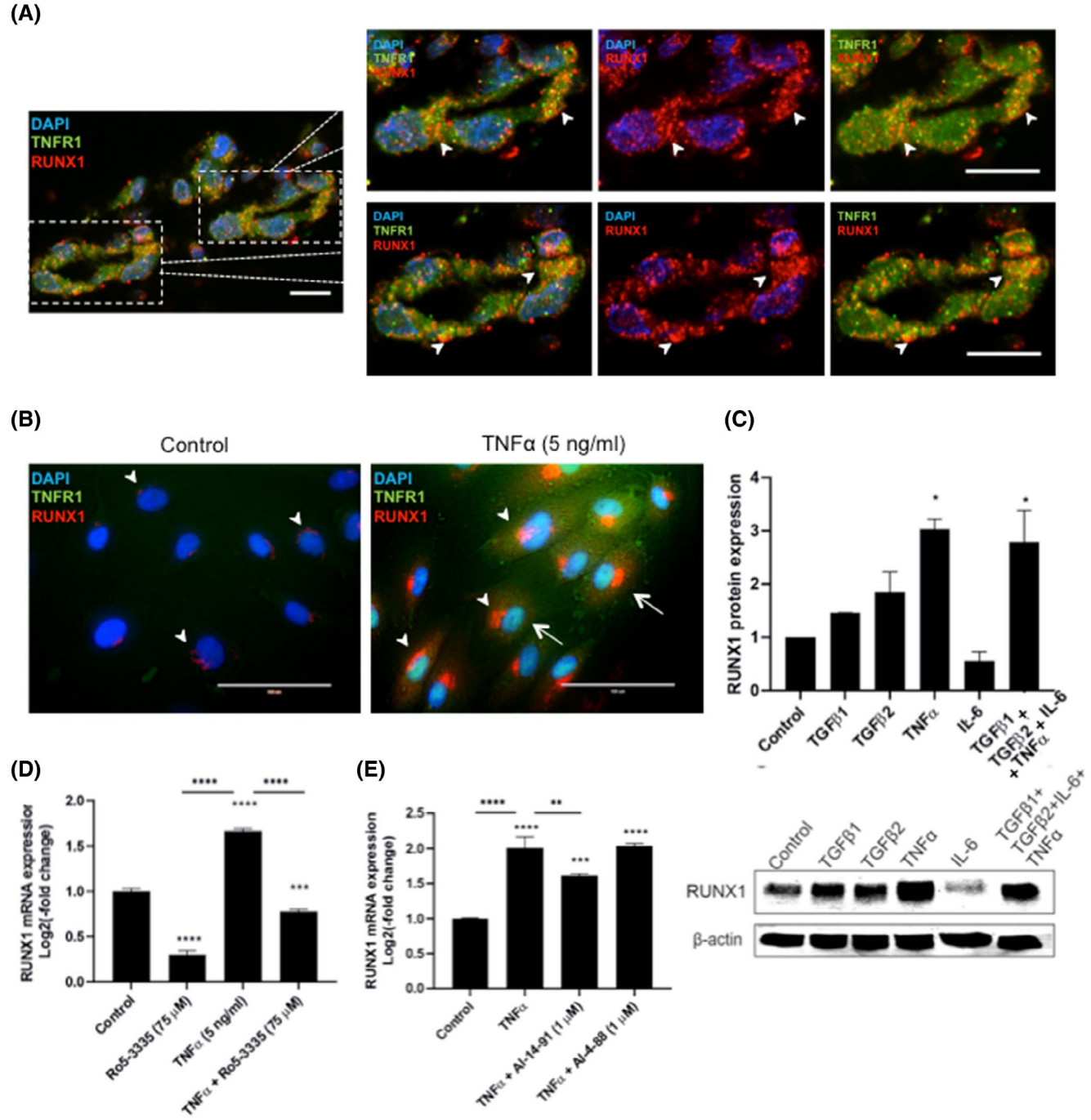

FIGURE 1 RUNX1 co-localized with TNFR1 while cytokines significantly increased RUNX1 expression and were reduced by RUNX1 inhibitors. (A) Representative images of IHC staining. A PDR patient-derived FVM sample was stained for DAPI (blue), TNFR1 (green), and RUNX1 (red). Visualization of perinuclear RUNX1 and TNFR1 co-staining (arrow heads) in the membrane vasculature. Scale bar 10 μM. (B) Representative images of ICC staining. HRMECs were stained for DAPI (blue), TNFR1 (green), and RUNX1 (red). Visualization of RUNX1 expression (arrow heads) and co-staining of TNFR1 (arrows) after stimulation with control media (left) or TNF-α (5 ng/mL) (right). All cells were stimulated with treatment media for 72 hours before being fixed. Scale bar 100 μM. (C) HRMECs were stimulated by cytokines TGFβ1 (5 ng/mL), TGFβ2 (5 ng/mL), TNF-α (5 ng/mL), IL-6 (5 ng/mL) and a combination of these cytokines (TGFβ1, TGFβ2, TNF-α and IL-6 5 ng/mL each) for 7 days (n = 2). (D) Quantitative RT-PCR for RUNX1 mRNA expression with small-molecule RUNX1 inhibitor Ro5-3335 (75 μM) after 48 hours of treatment (n = 6). (E) Quantitative RT-PCR for RUNX1 mRNA expression with small-molecule RUNX1 inhibitor AI-14-91 (1 μM) and inactive compound AI-4-88 after 48 hours of treatment (n = 6). qRT-PCR data are shown as ($\log_2$-(fold change)), normalized to endogenous HPRT expression and unstimulated control. Western blot analyses are normalized to β-actin and unstimulated control. Shown are mean values + SEM. Data are analyzed using one-way ANOVA with Dunnett's post hoc test. *$P < .05$; **$P < .01$; ***$P < .001$; ****$P < .0001$

increased RUNX1 expression in FVMs correlated with increased TNF Receptor 1 (TNFR1) expression, we evaluated the expression of RUNX1 (red) and TNFR1 (green) in the vasculature of a patient-derived FVM sample (Figure 1A). Both RUNX1 and TNFR1 expression was significantly increased in the vessels, compared to the surrounding tissue. A representative fundus photograph of a patient FVM is presented in Figure S1A, and patient demographic data are presented in Table S1. To determine relevance to other disease states, such as wet AMD, the expression of RUNX1 and TNFR1 in a mouse model of laser-induced choroidal neovascularization (CNV) was assessed and found to have co-expression of RUNX1 and TNFR1 within the CNV lesion. A representative image of a post-laser day 3 CNV lesion is shown in Figure S1B. To determine the effects of direct TNF-α stimulation on HRMECs, we evaluated the expression of RUNX1 and TNFR1 in HRMECs in control and TNF-α stimulated cells. Faint perinuclear RUNX1 (red) staining was observed in control (unstimulated) cells, while TNFR1 staining (green) revealed that low levels of TNFR1 are present in unstimulated HRMECs. Accumulation of RUNX1 was significantly increased in the cells after TNF-α stimulation for 3 days, as was the expression of TNFR1 in comparison to unstimulated control cells (Figure 1B). Further examination of RUNX1 localization through z-stack and single-slice confocal analysis indicates that RUNX1 is found both perinuclear and nuclear within HRMECs. Additionally, upon stimulation with TNF-α, RUNX1 expression increases both perinuclear and within the nucleus, indicating the activation of the transcription factor (Figure S1C). This was confirmed with a time-course analysis of the effects of TNF-α on the activation of RUNX1 via phosphorylation of RUNX1 (p-RUNX1). Protein expression of p-RUNX1 in stimulated endothelial cells was analyzed over 6 hours and found to significantly increase by 1 hour of stimulation and remain elevated across the analysis (Figure S1D).

3.2 | Pro-inflammatory cytokine TNF-α significantly increases RUNX1 expression

We next assessed RUNX1 expression in HRMECs by Western blot and quantitative RT-PCR (qRT-PCR). Pro-inflammatory mediators, such as TGFβ1, TGFβ2, TNF-α, and IL-6 have been implicated in retinal disease progression[10,13,37] and TNF-α has been identified as a biomarker of retinal diseases.[14] HRMECs were treated with TGFβ1, TGFβ2, TNF-α, IL-6 or combination treatment (TGFβ1, TGFβ2, TNF-α and IL-6, 5 ng/mL each). At day 7, RUNX1 protein expression was significantly upregulated 3-fold after TNF-α or combination treatment, as compared to control cells (Figure 1C). There was no significant increase in RUNX1 protein expression with TGFβ1, TGFβ2, or IL-6 stimulation alone. A time-course experiment demonstrated that RUNX1 mRNA levels peaked at 48 hours post-TNF-α stimulation, as assessed by qRT-PCR and presented in Figure S1E. RUNX1 mRNA expression was upregulated 2.3-fold compared to control, before rapidly declining at 72 hours, where it was not significantly different compared to controls. Taking advantage of this peak in RUNX1 expression, qRT-PCR analyses of TNF-α stimulated HRMECs were conducted at 48 hours, while RUNX1 protein levels, which are expected to increase after mRNA, were determined after 72 hours of treatment. To determine whether small-molecule RUNX1 inhibitors could counter the effects of TNF-α stimulation, Ro5-3335 (75 μM)[1] and AI-14-91 (1 μM)[36] were investigated. Basal RUNX1 mRNA expression was reduced significantly by 70% compared to control after Ro5-3335 treatment for 48 hours (Figure 1D), while co-treatment of TNF-α and Ro5-3335 induced a significant decrease in RUNX1 mRNA expression of 50% compared to TNF-α stimulated cells ($P < .0001$). Similarly, AI-14-91 significantly reduced RUNX1 mRNA expression levels from 2-fold (TNF-α stimulated cells) to 1.5-fold, while inactive control compound AI-4-88 was shown to have no effect on TNF-α-stimulated RUNX1 mRNA expression (Figure 1E). AI-14-91 also demonstrates a dose-dependent reduction in TNF-α-induced RUNX1 protein expression after 72 hours of treatment, presented in Figure S1F.

3.3 | JNK inhibitors abrogate the effect of TNF-α on RUNX1 expression

Next, we used specific pathway inhibitors to determine which TNF-α activated signaling pathway, NF-κB, JNK or p38/MAPK[38-40] was involved in the upregulation of RUNX1.[41-47] TNF-α stimulation for 48 hours causes a significant 2.3-fold increase in RUNX1 mRNA expression, while stimulation for 3 days causes a significant 2-fold increase in RUNX1 protein expression. To confirm our hypothesis that TNF-α is binding and signaling through TNFR1, we used a TNF-α-TNFR1 binding inhibitor, CAY10500, as a positive control. We then used PCR (Figure 2A) and Western blot (Figure 2B) analyses to measure RUNX1 expression levels when HRMECs were co-treated with TNF-α and a selective inhibitor [Caffeic acid phenethyl ester (CAPE) and Honokiol, NF-κB inhibitors; Withaferin A, a dual NF-κB/JNK inhibitor; SP600125 and TCS JNK 6o, JNK inhibitors; SB239063 and SB202190, p38/MAPK inhibitors]. A data table of these inhibitors is presented in Table S2. Only the dual NF-κB/JNK inhibitor Withaferin A, and the JNK inhibitors SP600125 and TCS JNK 6o efficiently blocked the up-regulation of RUNX1 expression by TNF-α. In contrast, inhibition of the NF-κB or p38/MAPK pathways did not alter the effect of TNF-α stimulation on RUNX1 mRNA and protein expression, compared to control. This suggested that TNF-α signaling stimulates RUNX1 expression through the JNK pathway.

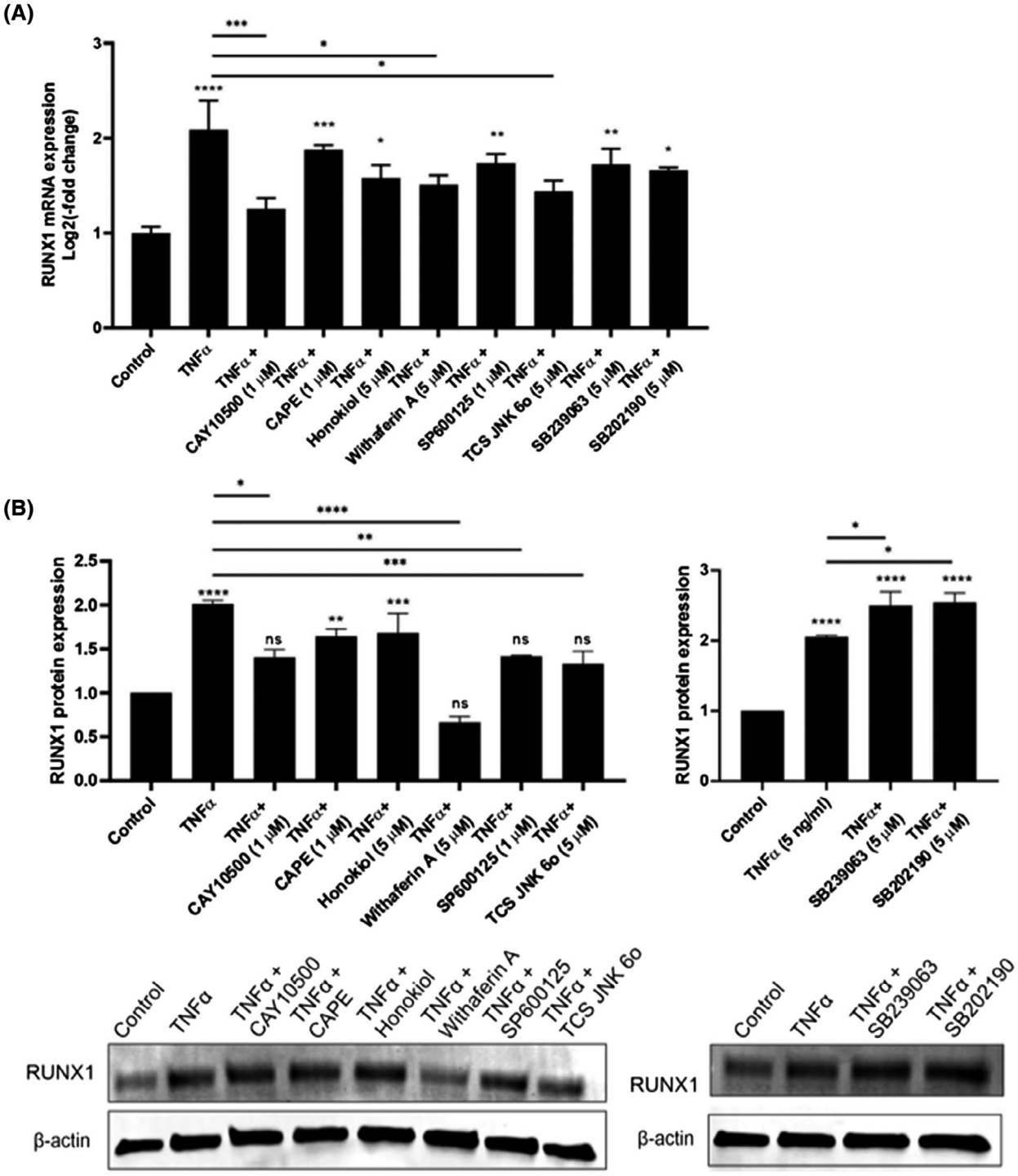

FIGURE 2 RUNX1 expression was reduced by blocking the TNF-α mediated JNK signaling pathway. Treatment of HRMECs with TNF-α (5 ng/mL) in combination with TNFR1 inhibitor, CAY10500 (1 μM); NF-κB inhibitors, CAPE (1 μM) and Honokiol (5 μM); dual NF-κB and JNK inhibitor, Withaferin A (5 μM); JNK inhibitors, SP600125 (1 μM) and TCS JNK 6o (5 μM) and p38/MAPK inhibitors, SB239063 (5 μM) and SB202190 (5 μM). Cells were treated for (A) 48 hours for quantification by qRT-PCR (n = 6) and (B) 72 hours for Western blot analyses (n = 2). qRT-PCR data are shown as (log_2-(fold change)), normalized to endogenous HPRT expression and unstimulated control. Western blot analyses are normalized to β-actin and unstimulated control. Shown are mean values + SEM. Data are analyzed using one-way ANOVA with Dunnett's post hoc test. *$P < .05$; **$P < .01$; ***$P < .001$; ****$P < .0001$

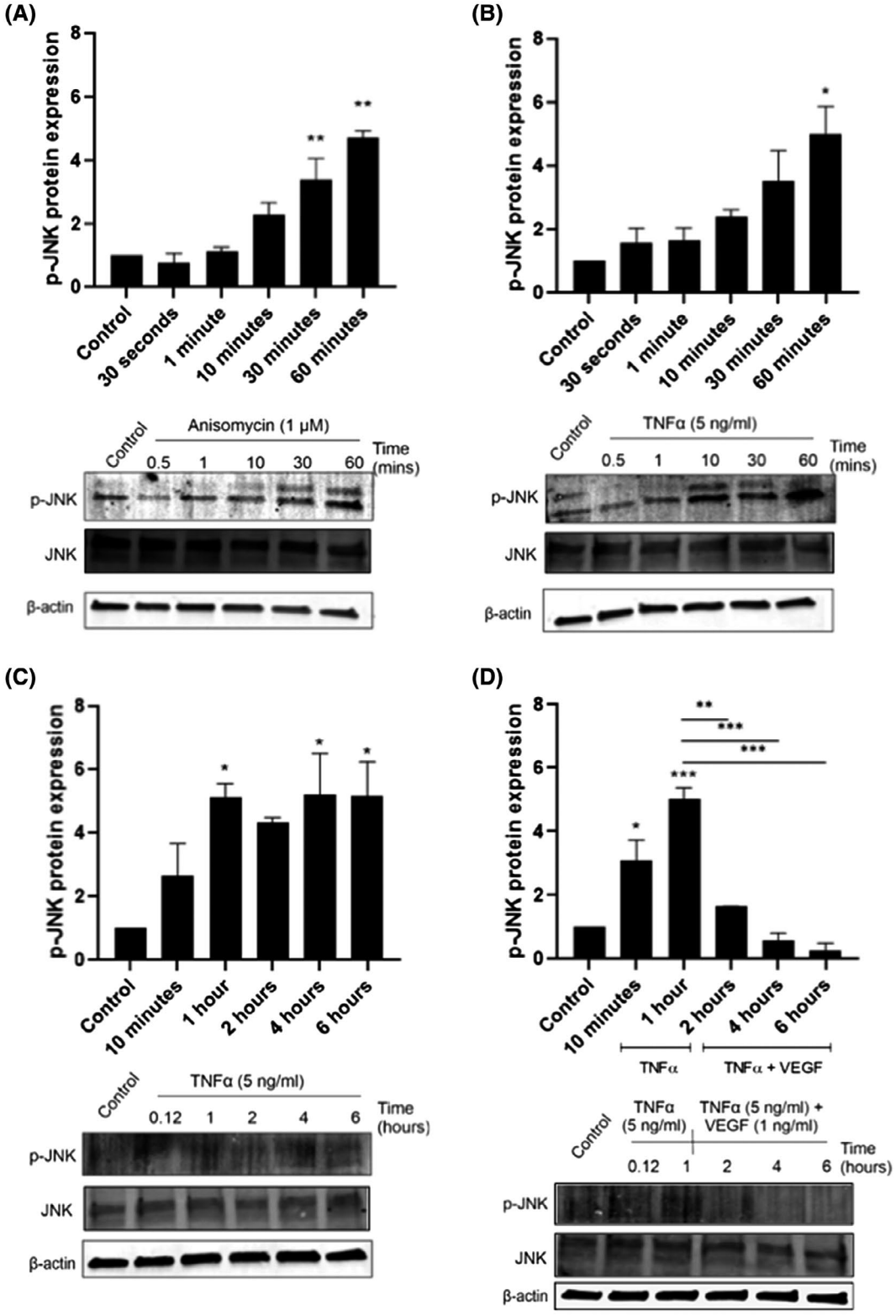

FIGURE 3 RUNX1 expression was regulated via p-JNK. HRMECs were treated with (A) direct JNK activator anisomycin (1 μM), or (B) TNF-α (5 ng/mL) for 30 seconds, 1 minute, 10 mins, 30 mins, and 60 mins. Results are normalized to untreated (control) lysates collected at 60 minutes (n = 2). (C) Six-hour time-course of HRMECs treated with TNF-α (5 ng/mL) with time points at 10 minutes, 1 hour, 2 hours, 4 hours, and 6 hours compared to control lysates, collected at 6 hours revealed significant activation of p-JNK from 1 to 6 hours (n = 2). (D) HRMECs were treated with TNF-α (5 ng/mL) for 1 hour, followed by the co-treatment of TNF-α (5 ng/mL) and VEGF (1 ng/mL) for the remaining 5 hours which revealed suppression of p-JNK with VEGF stimulation. Results are compared to control lysates collected at 6 hours (n = 2). Western blot analyses are normalized as (p-JNK/β-actin)/(JNK/β-actin) and further compared to unstimulated control. Shown are mean values + SEM. Data are analyzed using one-way ANOVA with Dunnett's post hoc test. *$P < .05$; **$P < .01$; ***$P < .001$; ****$P < .0001$

3.4 | TNF-α activates JNK kinase via activation of p-JNK

We also assessed whether TNF-α would affect the activation of JNK kinase via phosphorylation of JNK (p-JNK) in endothelial cells. TNF-α-mediated JNK activation has previously been shown to occur in fibroblasts.[48] Short time-course studies were employed to visualize these effects. The direct JNK activator, anisomycin (1 μM), which activates JNK through phosphorylation, was used as a positive control. We identified significantly increased p-JNK expression normalized to total JNK expression 30 minutes after HRMEC stimulation with anisomycin (Figure 3A). Stimulation with TNF-α (Figure 3B) also significantly increased p-JNK activation by 1 hour of treatment. It has been reported previously that VEGF can act as a suppressor of JNK, by inhibiting its phosphorylation.[49] To determine its effect in HRMECs, we investigated the peak of p-JNK stimulation caused by TNF-α and determined that it peaked at 1 hour and was sustained over a 6-hour time-course (Figure 3C). After TNF-α stimulation for 1 hour, HRMECs were co-treated with TNF-α+ VEGF (5 and 1 ng/mL) from hours 1 to 6. This time-course study demonstrated the rapid and potent effects of VEGF on the inhibition of p-JNK phosphorylation (Figure 3D).

3.5 | TNF-α and D-glucose co-treatment induce additive RUNX1 expression, while exogenous VEGF decreases RUNX1 expression

Although TNF-α is highly expressed in several pathological retinal diseases, we know from our[1] and other[2] studies that D-glucose is also able to induce the up-regulation of RUNX1 expression in both PDR membranes and in HRMECs. We replicated these experiments using D-glucose as the stimulus and found that D-glucose stimulates an increase in both RUNX1 mRNA and protein expression by 1.3-fold at 48 hours. This increase can be modulated by JNK inhibitors Withaferin A and TCS JNK 6o, in a dose-dependent manner, similar to that seen for TNF-α (Figure 4A, B). These data suggest that both TNF-α and D-glucose are able to induce RUNX1 expression through p-JNK activation.

As shown in Figure 3 above, we found that VEGF suppresses TNF-α stimulated p-JNK activation, suggesting that VEGF would suppress RUNX1 expression. Accordingly, we investigated whether the downregulation of p-JNK protein expression by VEGF had a downstream effect on RUNX1 expression. VEGF suppressed TNF-α induced RUNX1 protein expression in a dose-dependent fashion (Figure 4C). Additionally, this co-treatment caused a dose-dependent reduction in both RUNX and JNK1 mRNA expression (Figure S2A and B, respectively). Similar VEGF-driven dose-dependent results were seen when D-glucose was used as the stimulus after 48 hours of treatment (Figure 4D).

We next tested our hypothesis that TNF-α and D-glucose can additively stimulate the expression of RUNX1. Co-stimulation of HRMECs with TNF-α+ D-glucose caused a significant ($P < .0001$) 3.3-fold increase in RUNX1 protein expression, which was greater than the increases seen after 3 days by TNF-α or D-glucose stimulation alone. To determine the effect that the lowest significant concentration of VEGF would have on this system, exogenous VEGF (0.1 ng/mL) was added to TNF-α+ D-glucose. In this analysis, RUNX1 levels were reduced so as to be non-significant to TNF-α treatment, although this still represents a significant 2.5-fold increase in RUNX1 levels compared to unstimulated control cells. Similar patterns of expression are seen in both mRNA (Figure S2C) and protein analyses (Figure 4E). Osmotic controls undertaken with $_{L}$-glucose and mannitol demonstrate no significant changes in RUNX1 expression compared to control-treated cells (Figure S2D). Additionally, investigations into the effects of the anti-VEGF drug aflibercept on RUNX1 expression, indicated that at a concentration of 1 μg/μL, RUNX1 expression was increased significantly compared to control-treated cells (Figure S2E). When HRMECs were treated with a combination of TNF-α+ aflibercept at a concentration of 1 μg/μL, a significant increase was seen in RUNX1 mRNA expression compared to TNF-α stimulated cells alone (Figure S2F).

We also determined RUNX1 expression via ICC staining of HMRECs after TNF-α, VEGF, D-glucose or combination stimulation for 72 hours (Figure 4F). No clear differences in staining are seen in the accumulation of RUNX1 (red) between untreated cells, VEGF (1 ng/mL), and TNF-α+ VEGF co-treated cells. However, there are evident differences in RUNX1 staining between control and TNF-α stimulated cells, where there is significant perinuclear RUNX1 accumulation. Similarly, clear differences in staining are seen between control and D-glucose stimulated cells. Stimulation of HRMECs with TNF-α+ D-glucose co-treatment appears to show a more distinct staining pattern with very high levels of both perinuclear RUNX1 accumulation as well as more diffuse RUNX1 staining throughout the cells.

3.6 | Identification of the JNK activation of AP-1 as a mediator of RUNX1 expression

As we have shown that the stimulation of HRMECs with TNF-α leads to a signaling pathway through JNK and results in a significant increase in RUNX1 expression, we attempted to determine whether a feedback loop was involved as well as potential points of inhibition. It is known that JNK signals Activator Protein 1 (AP-1)[50] and that certain leukemic RUNX1-fusion proteins can signal back through JNK.[51] Inhibition of AP-1 with SR11302 (1 μM) alone showed no significant change in mRNA expression; however,

co-treatment of TNF-α and SR11302 resulted in significant decreases in RUNX1 mRNA expression ($P < .05$) compared to TNF-α as a positive control (Figure 5A). SR11302 inhibition also caused a significant reduction in RUNX1 protein expression (Figure S3A). In addition, SR11302 caused a significant reduction in JNK1 mRNA expression during co-treatment with both TNF-α and anisomycin (Figure 5B). Inhibition of RUNX1 driven transcription with Ro5-3335 in conjunction with TNF-α or anisomycin stimulation, caused a significant decrease in RUNX1 (Figure 5C) and JNK1 (Figure 5D) mRNA expression, suggesting the RUNX1 regulation of JNK1 expression.

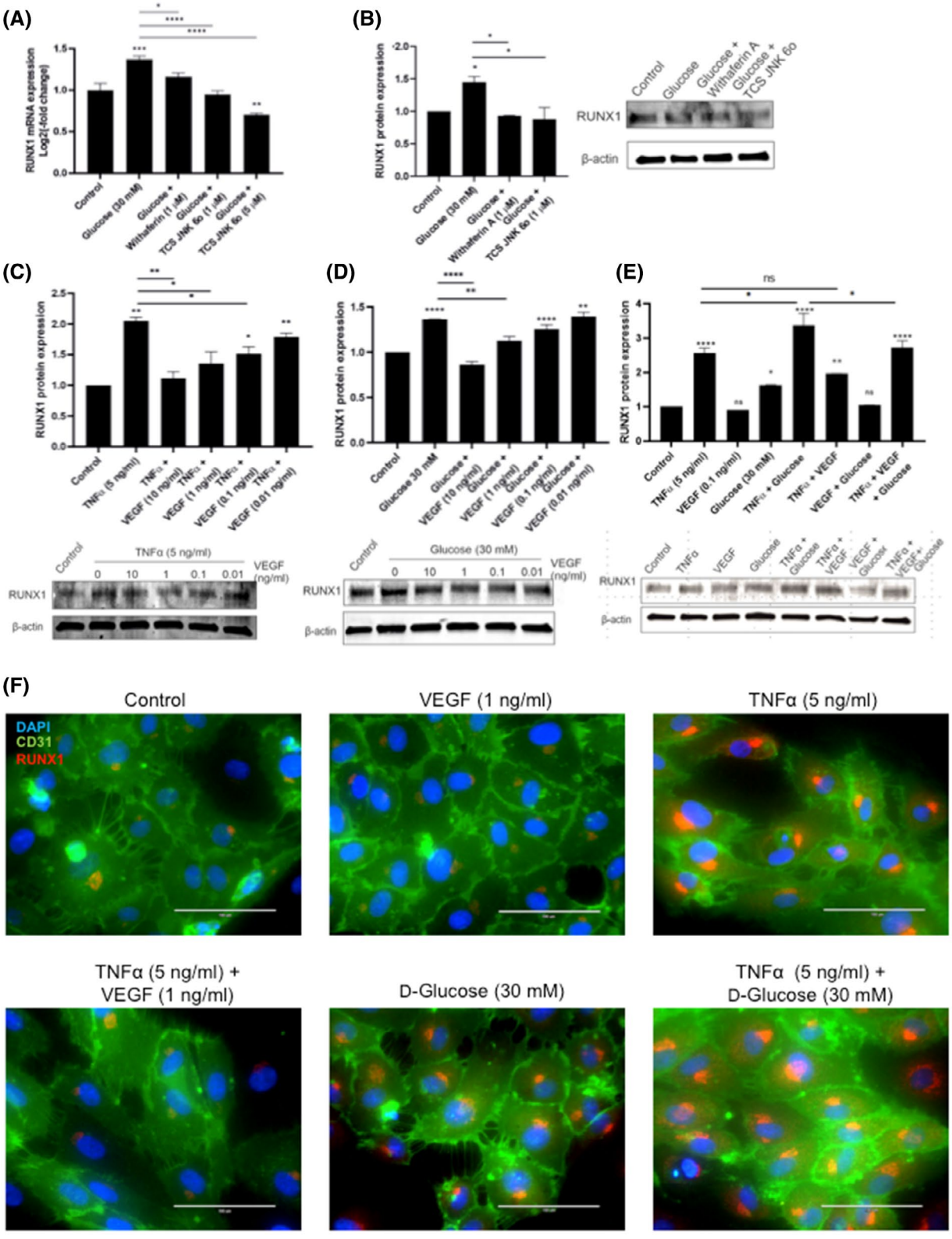

FIGURE 4 Addition of exogenous VEGF caused a dose-dependent decrease in RUNX1 expression, while TNF-α and D-glucose caused additive increases in the levels of RUNX1 expression. (A) Quantitative RT-PCR for RUNX1 mRNA expression with D-glucose (30 mM) and inhibitors Withaferin A (1 μM) and TCS JNK 6o (1 μM and 5 μM) (n = 6). (B) HRMECs were treated with D-glucose (30 mM) in combination with inhibitors Withaferin A (1 μM) and TCS JNK 6o (1 μM) for 48 hours (n = 2). (C,D) Cells were co-treated with (C) TNF-α (5 ng/mL) and VEGF (10–0.01 ng/mL) for 72 hours (n = 2) and (D) D-glucose (30 mM) and VEGF (10–0.01 ng/mL) for 48 hours (n = 2) for Western blot analyses. (E) HRMECs were treated for 72 hours with control media (unstimulated cells), TNF-α (5 ng/mL), VEGF (0.1 ng/mL), D-glucose (30 mM), TNF-α + D-glucose, TNF-α + VEGF, D-glucose + VEGF, and TNF-α + VEGF+ D-glucose and analyzed for RUNX1 protein expression. qRT-PCR data are shown as (log_2-(fold change)), normalized to endogenous HPRT expression and unstimulated control. Western blot analyses are normalized to β-actin and unstimulated control. Shown are mean values + SEM. Data are analyzed using one-way ANOVA with Dunnett's post hoc test. *$P < .05$; **$P < .01$; ***$P < .001$; ****$P < .0001$. (F) Representative images of ICC staining. Cells were stained for DAPI (blue), CD31 (green), and RUNX1 (red). RUNX1 expression after treatment with (from top left) control (unstimulated cells), VEGF (1 ng/mL), TNF-α (5 ng/mL), TNF-α + VEGF, D-glucose (30 mM), TNF-α + D-glucose. Scale bar 100 μM. All cells were stimulated with treatment media for 72 hours before being fixed

3.7 | TNF-α stimulation of endothelial cells has no effect on cell proliferation, but induces cell migration

It is known that TNF-α has contradictory effects on angiogenesis in vitro and in vivo.[12] To investigate TNF-α stimulation in HRMECs, we performed a cell proliferation experiment (Figure 6A). No significant difference in LDH levels was seen after 48 hours of treatment compared to control (Figure S3B). With constant stimulation over 48 hours, VEGF significantly increased cell proliferation, while TNF-α showed no change compared to control cells, despite its known effects on RUNX1 expression. However, in a pre-primed cell migration system, quantification of wound closure 12 hours after scratch initiation indicated that TNF-α and VEGF both alone and in combination demonstrated significantly increased cell migration compared to unstimulated control cells ($P < .05$; Figure 6B).[11] VEGF and TNF-α increased migration by 1.5 times each, while in combination, migration was increased 1.6 times. The RUNX1 inhibitors AI-14-91 and Ro5-3335 acted as a negative control to inhibit wound closure,[1] while TCS JNK 6o also significantly inhibited HRMEC migration. Both inhibitors reduced cell migration by 40% compared to untreated cells.

4 | DISCUSSION

TNF-α is reported to be present at elevated levels in several blinding eye diseases involving the retina. These include proliferative diabetic retinopathy (PDR),[14,22] wet age-related macular degeneration (wet-AMD) [17-19] and retinopathy of prematurity (ROP).[20,21] We have previously identified RUNX1 as a potent mediator of retinal angiogenesis in disease states such as PDR[1]; however, the pathways activated by diabetic retinopathy-related stimuli, which result in RUNX1 upregulation in HRMECs, are poorly understood. Understanding the molecular mechanisms which contribute to the upregulation of RUNX1 expression is necessary to aid in the development of targeted treatments for retinopathy.

In the present study, we evaluated the effects of both the pro-inflammatory cytokine TNF-α and high levels of D-glucose on RUNX1 expression. Investigations into the levels of RUNX1 and TNFR1 found in patient-derived FVMs demonstrated strong co-expression within the vasculature. Similarly, we found co-expression of RUNX1 and TNFR1 in a mouse model of laser-induced CNV, indicating RUNX1 involvement in other pathologic conditions, such as wet AMD. Stimulation of HRMECs with TNF-α also resulted in a significant increase in RUNX1 and TNFR1 expression. We additionally determined that this increase in RUNX1 expression is due to the TNF-α activation of RUNX1 through nuclear localization and phosphorylation of the transcription factor. The reported data also show that two small-molecule RUNX1 inhibitors, Ro5-3335 and AI-14-91, demonstrate highly effective inhibition of RUNX1 mRNA and protein expression in the presence of TNF-α. Ro5-3335 also significantly inhibits RUNX1 mRNA expression alone, which leads us to conclude that as RUNX1 inhibition results in reduced RUNX1 expression, RUNX1 is at least in part responsible for its own transcription.[52]

TNF-α is known to signal through three main signaling pathways, NF-κB, JNK, and p38/MAPK [27]; however, the pathway, and the response, differ based on cell type[53,54] so system-wide effects may utilize more than one pathway. Our results show that HRMECs simultaneously stimulated with TNF-α and p38/MAPK or NF-κB pathway inhibitors showed no significant reductions in RUNX1 expression. However, TNF-α inhibition with dual NF-κB/JNK inhibitor Withaferin A, or JNK inhibitors SP600125 and TCS JNK 6o, caused significant reductions in RUNX1 mRNA and protein expression. We further determined by time-course studies that expression of the activated form of JNK, p-JNK, can be stimulated with direct JNK activator anisomycin[55] within 30 minutes of treatment. We also determined that TNF-α signals through JNK and can activate p-JNK within an hour of treatment. We additionally investigated the role of VEGF, a

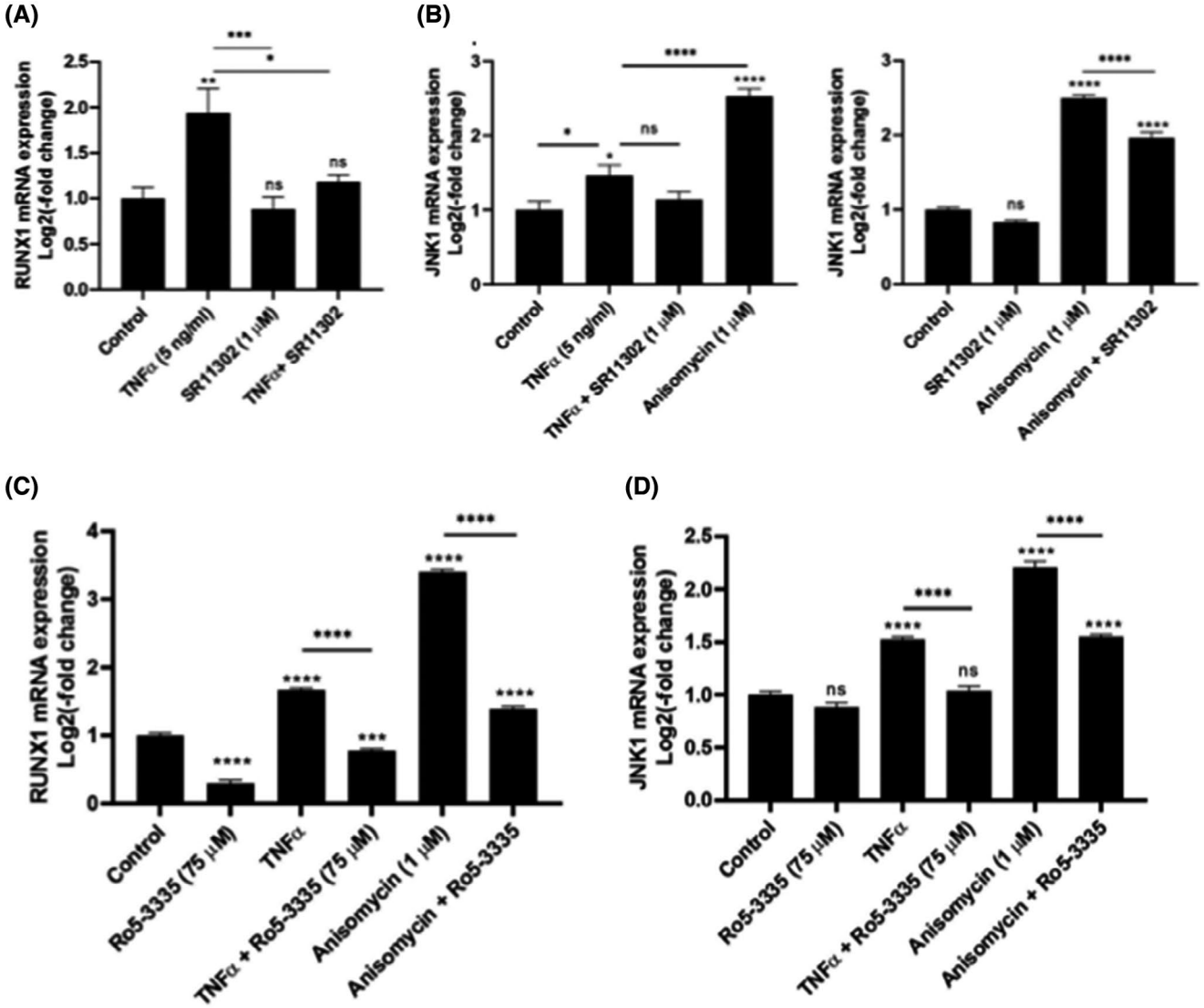

FIGURE 5 JNK regulated RUNX1 expression through AP1, and JNK expression is mediated by RUNX1 in a feedback loop. (A) qRT-PCR for RUNX1 expression using small-molecule AP-1 inhibitor SR11302 (1 μM) in combination with TNF-α (5 ng/mL) stimulated for 48 hours with treatment (n = 6). (B) qRT-PCR for JNK1 mRNA expression. Direct JNK activator anisomycin (1 μM) acts as a positive control for initiating JNK1 mRNA (n = 6). (C, D) qRT-PCR analyzing the effects of RUNX1 inhibitor Ro5-3335 (75 μM) with TNF-α (5 ng/mL) or anisomycin (1 μM) on (C) RUNX1 and (D) JNK1 mRNA expression (n = 6). qRT-PCR data are shown as (log_2-(fold change)), normalized to endogenous HPRT expression and unstimulated control. Shown are mean values + SEM. Data are analyzed using one-way ANOVA with Dunnett's post hoc test. *$P < .05$; **$P < .01$; ***$P < .001$; ****$P < .0001$

known and potent factor in angiogenesis, in this system. With TNF-α stimulation, p-JNK expression remains increased over the 6-hour time-course; however, the phosphorylation of JNK is inhibited by the addition of exogenous VEGF. Levels of p-JNK were downregulated over 6 hours, indicating that the action of VEGF is likely to occur through the inhibition of JNK activation.[49]

We know from our previous work that RUNX1 mRNA and protein expression in HRMECs increases upon stimulation with high glucose.[1] Others[2] have shown that RUNX1 upregulation caused by D-glucose stimulation can be mediated by the p38 pathway and here, we used inhibitors of TNF-α induced RUNX1 expression to show a secondary pathway through which RUNX1 levels stimulated by high glucose can be mediated. Addition of JNK inhibitors to HRMECs stimulated with D-glucose caused significant reductions in RUNX1 expression at both the mRNA and protein levels. D-glucose was also found to significantly increase p-JNK activation over an hour. Taken together, this indicates that both TNF-α and D-glucose regulate and stimulate RUNX1 expression through the JNK pathway and that this stimulation can be effectively blocked by JNK inhibitors. Further to this, we examined the role of VEGF in the regulation of RUNX1 expression, where we have determined the dose-dependent suppression of RUNX1 expression by VEGF in the presence of both TNF-α and D-glucose. We believe that the ability of

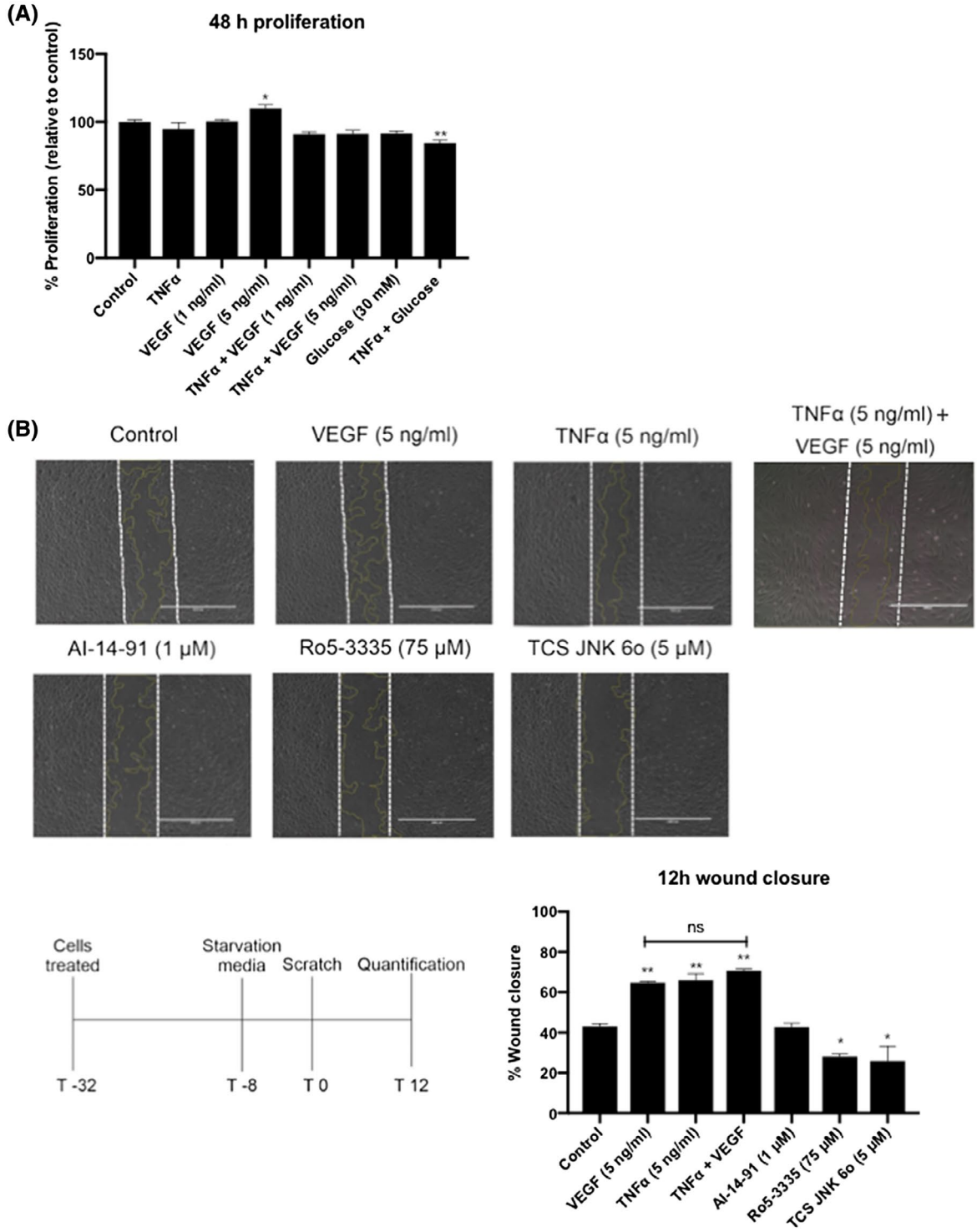

FIGURE 6 Proliferation and scratch wound healing were affected by RUNX1 activation. (A) Cell proliferation was analyzed after 48 hours of treatment with TNF-α (5 ng/mL), VEGF (1 ng/mL), VEGF (5 ng/mL), TNF-α + VEGF (1 ng/mL), TNF-α + VEGF (5 ng/mL), D-glucose (30 mM) and TNF-α + D-glucose treatments compared to untreated control cells (n = 8). (B) HRMEC scratch wound assays were analyzed for wound closure at 12 hours postscratch. HRMECs were treated (from top left) with control media, VEGF (5 ng/mL), TNF-α (5 ng/mL), TNF-α + VEGF (5 ng/mL), AI-14-91 (1 μM), Ro5-3335 (75 μM) or TCS JNK 6o (5 μM). Scale bar 1000 μm. White dotted lines indicate original scratch wound area, yellow lines indicate healed areas (experiment performed in duplicate). Results are normalized to unstimulated control. Shown are mean values + SEM. Data are analyzed using one-way ANOVA with Dunnett's post hoc test. $*P < .05$

VEGF to reduce RUNX1 expression is due to its actions on JNK and the inhibition of its phosphorylation.[49] In addition, several other articles have identified that VEGF may promote angiogenesis by stimulating cell proliferation, but also by acting as a cell survival mechanism and inhibiting endothelial cell apoptosis.[56,57] We reasoned that in the presence of

TNF-α and absence of exogenous VEGF, RUNX1 promotes cell survival and prevents apoptosis in HRMECs.[58]

Levels of TNF-α and D-glucose[14,15,59] as well as levels of VEGF[37] are known to be elevated in the eyes of patients with PDR, among other proliferative retinal diseases, establishing why anti-VEGF agents are a common therapeutic option.[24] We show that RUNX1 levels are suppressed by VEGF in the presence of TNF-α or D-glucose alone, suggesting that RUNX1 may work as a pathologic angiogenic pathway through a different mechanism to that of VEGF. We demonstrate that HRMECs treated with a combination of TNF-α and D-glucose are subjected to an additive effect on the resulting expression of RUNX1 even in the presence of VEGF. Osmotic controls undertaken with L-glucose and mannitol demonstrate no significant changes in RUNX1 expression compared to control-treated cells, indicating that changes in RUNX1 expression levels are not due to the osmolarity of the solution. This indicates that PDR, where both TNF-α and D-glucose are highly elevated within the eye, RUNX1 is elevated even in the presence of elevated VEGF. As RUNX1 is affected by both stimuli (TNF-α and D-glucose) in an additive fashion, it is likely to play a significant role in the progressive pathology of PDR. These results suggest the role of improved glucose control or inhibition of TNF signaling pathways in the management of DR (Figure 7A). Further, these data suggest that in certain cases, anti-VEGF agents may worsen PDR[60,61] due to the uncontrolled upregulation of RUNX1. It was determined here that the use of anti-VEGF agent aflibercept, can cause a significant increase in the expression of RUNX1 mRNA. Additionally, when HRMECs are treated with aflibercept in conjunction with TNF-α, a significant increase in RUNX1 mRNA expression is seen. Thus, our work suggests an important role for combined anti-VEGF and RUNX1 inhibition treatment for the management of PDR (Figure 7A).

A recent study identified that p-JNK can activate the oncoprotein c-Jun, which dimerizes with c-Fos to form the activator protein-1 (AP-1) transcription factor.[50] Inhibition of AP-1 with SR11302[62] demonstrated similar results to that seen when using the RUNX1 small-molecule

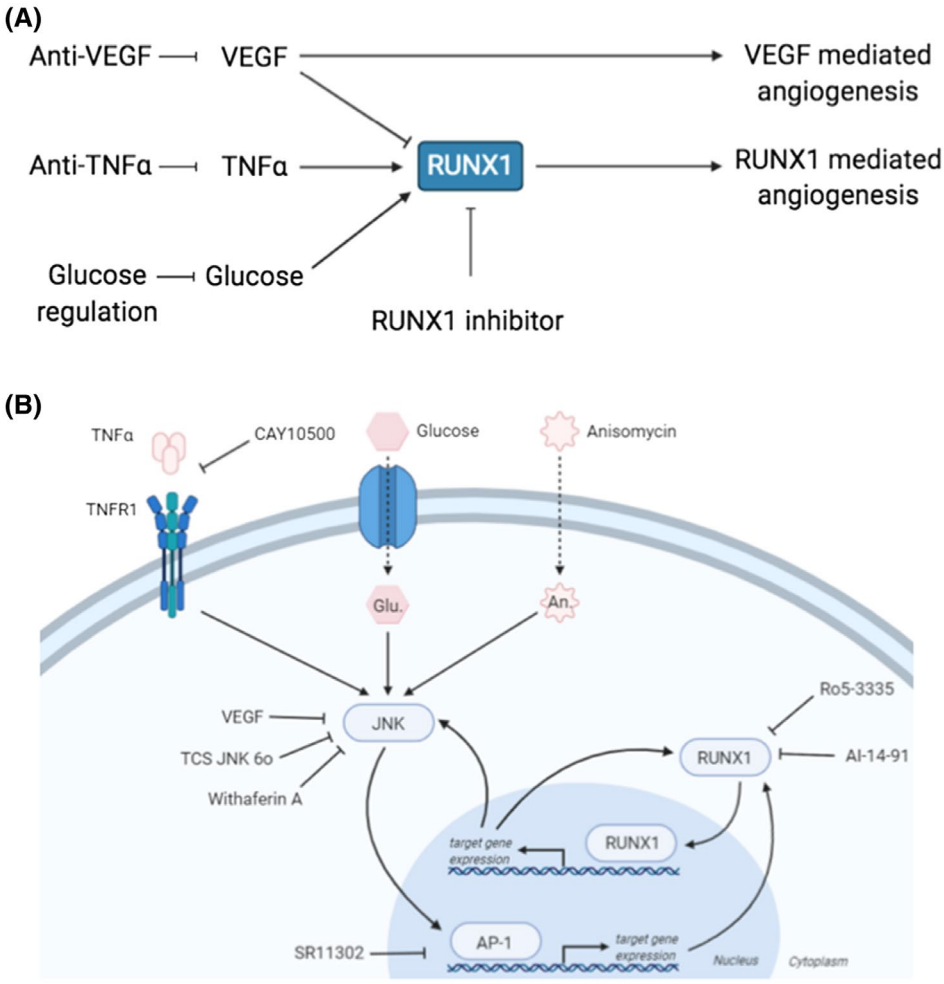

FIGURE 7 TNF-α-JNK-RUNX1 pathway. A, Schematic indicating the potential of a combined anti-VEGF/anti-RUNX1 therapy on the treatment of pathologic angiogenesis, (B, Schematic of the basic TNF-α-JNK-RUNX1 pathway, including the actions of D-glucose and anisomycin on JNK and the actions of named inhibitors, which have been identified as causing changes in RUNX1 expression levels

inhibitors Ro5-3335 and AI-14-91, indicating that the AP-1 transcription factor is important in TNF-α-stimulated RUNX1 upregulation.[50] We also identified that the inhibition of RUNX1 leads to a significant reduction in the expression of JNK1 mRNA, demonstrating that a regulatory loop exists from RUNX1 to JNK. In a previous report on leukemogenesis in acute myeloid leukemia (AML) cells, RUNX1 fusion protein, AML1-ETO, trans-activates the c-jun promoter through AP-1 by activating the JNK pathway in AML cells.[51] Furthermore, this present study identifies that unmodified RUNX1 can initiate this feedback loop from RUNX1 to JNK in primary cells and the feedback loop can further be modulated by small-molecule inhibitors of JNK, AP-1 or RUNX1 (Figure 7B).

In functional assays with VEGF as a positive control, TNF-α showed no difference to control cells in the proliferation of HRMECs over 48 hours. This is not unexpected due to some contention over the role of TNF-α in in vitro angiogenesis.[12] However, both VEGF and TNF-α, alone and in combination, are shown to increase the migration of HRMECs over 12 hours.[11] This indicates the breadth of factors responsible for cell migration, aside from RUNX1. With regards to inhibition, RUNX1 inhibitors AI-14-91 and Ro5-3335 and JNK inhibitor, TCS JNK 6o, significantly reduce the migration of cells further confirming the importance of RUNX1 as a mediator of endothelial cell function.

In conclusion, we have identified the link between the pro-inflammatory cytokine TNF-α, high levels of D-glucose, and the increased expression and activation of transcription factor RUNX1. These studies further support our hypothesis that RUNX1 is significantly involved in the progression of PDR, and potentially other diseases of pathologic angiogenesis. We have identified that in HRMECs, the TNF-α- or D-glucose-RUNX1 signaling pathways are mediated through JNK and this then leads to a JNK-AP-1-RUNX1 signal transduction feedback loop, which causes upregulation of RUNX1 expression. Using small-molecule inhibitors of JNK, AP-1, and RUNX1, we have demonstrated that the effects of TNF-α and D-glucose stimulation on RUNX1 expression can be successfully modulated. As both TNF-α, D-glucose, and by extension RUNX1 have an important role in the development and progression of PDR and other diseases of aberrant ocular angiogenesis, this link may have significant therapeutic implications in the identification of future therapeutic targets.

ACKNOWLEDGMENTS

Research reported in this publication was supported by the National Eye Institute of the National Institutes of Health under award number: R01EY027739 (L. A. K), the E. Matilda Zieger Foundation for the Blind (L. A. K), the Karl Kirchgessner Foundation (L. A. K), Michel Plantevin (L. A. K) and the National Cancer Institute of the National Institutes of Health under award number: R01CA234478 (J. H. B).

CONFLICT OF INTEREST

L. A. Kim and J. F. Arboleda-Velasquez have filed a patent for the treatment of aberrant angiogenesis via RUNX1 modulation.

AUTHOR CONTRIBUTIONS

H. A. B. Whitmore, L. A. Kim and J. F. Arboleda-Velasquez designed research; H. A. B. Whitmore, D. Amarnani, M. O'Hare, and M. An performed research; L. Gonzalez-Buendia and S. Delgado-Tirado provided technical assistance; J. Pedron and J. H. Bushweller contributed new reagents or analytical tools; H. A. B. Whitmore analyzed data; H. A. B. Whitmore wrote the paper; J. Pedron, J. H. Bushweller, L. A. Kim and J. F. Arboleda-Velasquez edited and provided comments on the paper.

REFERENCES

1. Lam JD, Oh DJ, Wong LL, et al. Identification of RUNX1 as a mediator of aberrant retinal angiogenesis. *Diabetes*. 2017;66:1950-1956.
2. Zou W, Zhang Z, Luo S, et al. p38 promoted retinal micro-angiogenesis through up-regulated RUNX1 expression in diabetic retinopathy. *Biosci Rep*. 2020;BSR20193256.
3. Mintz-Hittner HA, Kennedy KA, Chuang AZ. Efficacy of intravitreal bevacizumab for stage 3+ retinopathy of prematurity. *N Engl J Med*. 2011;364:603-615.
4. Grunwald JE, Daniel E, Huang J, et al. Risk of geographic atrophy in the comparison of age-related macular degeneration treatments trials. *Ophthalmol*. 2014;121:150-161.
5. Miller JW, Adamis AP, Aiello LP. Vascular endothelial growth factor in ocular neovascularization and proliferative diabetic retinopathy. *Diabetes Metab Rev*. 1997;13:37-50.
6. Sato T, Wada K, Arahori H, et al. Serum concentrations of bevacizumab (avastin) and vascular endothelial growth factor in infants with retinopathy of prematurity. *Am J Ophthalmol*. 2012;153:327-333.
7. Lepore D, Quinn GE, Molle F, et al. Intravitreal bevacizumab versus laser treatment in type 1 retinopathy of prematurity: report on fluorescein angiographic findings. *Ophthalmol*. 2014;121:2212-2219.
8. Gross JG, Glassman AR, Jampol LM, et al. Panretinal photocoagulation vs intravitreous ranibizumab for proliferative diabetic retinopathy: a randomized clinical trial. *JAMA*. 2015;314:2137-2146.
9. Carswell EA, Old LJ, Kassel RL, Green S, Fiore N, Williamson B. An endotoxin-induced serum factor that causes necrosis of tumors. *PNAS*. 1975;72:3666-3670.
10. Krishnaswamy G, Kelley JL, Yerra L, Smith JK, Chi DS. Human endothelium as a source of multifunctional cytokines: molecular regulation and possible role in human disease. *J Interferon Cytokine Res*. 1999;19:91-104.
11. Sainson RCA, Johnston DA, Chu HC, et al. TNF primes endothelial cells for angiogenic sprouting by inducing a tip cell phenotype. *Blood*. 2008;111:4997-5007.
12. Frater-Schroder M, Risau W, Hallmann R, Gautschi P, Bohlen P. Tumor necrosis factor type alpha, a potent inhibitor of endothelial cell growth in vitro, is angiogenic in vivo. *PNAS*. 1987;84:5277-5281.
13. Fajardo LF, Kwan HH, Kowalski J, Prionas SD, Allison AC. Dual role of tumor necrosis factor-alpha in angiogenesis. *Am J Pathol*. 1992;140:539-544.

14. Costagliola C, Romano V, De Tollis M, et al. TNF-alpha levels in tears: a novel biomarker to assess the degree of diabetic retinopathy. *Mediators Inflamm*. 2013;2013:629529.
15. Hernandez C, Simo-Servat A, Bogdanov P, Simo R. Diabetic retinopathy: new therapeutic perspectives based on pathogenic mechanisms. *J Endocrinol Inv*. 2017;40:925-935.
16. Huang H, Gandhi JK, Zhong X, et al. TNFα is required for late BRB breakdown in diabetic retinopathy, and its inhibition prevents leukostasis and protects vessels and neurons from apoptosis. *IOVS*. 2011;52:1336-1344.
17. Fernández-Vega B, Fernández-Vega Á, Rangel CM, et al. Blockade of Tumor Necrosis Factor-Alpha: a role for Adalimumab in neovascular age-related macular degeneration refractory to anti-angiogenesis therapy? *Case Rep Ophthalmol*. 2016;7:154-162.
18. Ishikawa M, Jin D, Sawada Y, Abe S, Yoshitomi T. Future therapies of wet age-related macular degeneration. *J Ophthalmol*. 2015;2015:138070.
19. Sato T, Takeuchi M, Karasawa Y, Enoki T, Ito M. Intraocular inflammatory cytokines in patients with neovascular age-related macular degeneration before and after initiation of intravitreal injection of anti-VEGF inhibitor. *Sci Rep*. 2018;8:1-10.
20. Hellgren G, Löfqvist C, Hansen-Pupp I, et al. Increased postnatal concentrations of pro-inflammatory cytokines are associated with reduced IGF-I levels and retinopathy of prematurity. *Growth Horm IGF Res*. 2018;39:19-24.
21. Rivera JC, Holm M, Austeng D, et al. Retinopathy of prematurity: inflammation, choroidal degeneration, and novel promising therapeutic strategies. *J Neuroinflamm*. 2017;14:1-14.
22. Huang H, Li W, He J, Barnabie P, Shealy D, Vinores SA. Blockade of Tumor Necrosis Factor alpha prevents complications of diabetic retinopathy. *J Clin Exp Ophthalmol*. 2014;5:1-12.
23. Simo-Servat O, Simo R, Hernandez C. Circulating biomarkers of diabetic retinopathy: an overview based on physiopathology. *J Diabetes Res*. 2016;3:1-13.
24. Amin RH, Frank RN, Kennedy A, Eliott D, Puklin JE, Abrams GW. Vascular endothelial growth factor is present in glial cells of the retina and optic nerve of human subjects with nonproliferative diabetic retinopathy. *IOVS*. 1997;38:36-47.
25. Limb GA, Chignell AH, Woon H, Green W, Cole CJ, Dumonde DC. Evidence of chronic inflammation in retina excised after relaxing retinotomy for anterior proliferative vitreoretinopathy. *Graefes Arch Clin Exp Ophthalmol*. 1996;234:213-220.
26. Aiello LP, Avery RL, Arrigg PG, et al. Vascular endothelial growth factor in ocular fluid of patients with diabetic retinopathy and other retinal disorders. *N Engl J Med*. 1994;331:1480-1487.
27. Sabio G, Davis RJ. TNF and MAP kinase signalling pathways. *Semin Immunol*. 2014;26:237-245.
28. Spandau U, Kim SJ. Recurrence of ROP After Anti-VEGF Treatment. In *Pediatric Retinal Vascular Disease: From Angiograpy to Vitrectomy*. Berlin, Heidelburg: Springer; 2019:149-152.
29. Mason JO, Nixon PA, White MF. Intravitreal injection of bevacizumab (Avastin) as adjunctive treatment of proliferative diabetic retinopathy. *Am J Ophthalmol*. 2006;142:685-688.
30. The Diabetic Retinopathy Study Research Group. Photocoagulation treatment of proliferative diabetic retinopathy. Clinical application of Diabetic Retinopathy Study (DRS) findings, DRS Report Number 8. *Ophthalmol*. 1981;88:583-600.
31. Bressler SB, Beaulieu WT, Glassman AR, et al. Diabetic retinopathy clinical research N. factors associated with worsening proliferative diabetic retinopathy in eyes treated with panretinal photocoagulation or ranibizumab. *Ophthalmol*. 2017;124:431-439.
32. Brown DM, Kaiser PK, Michels M, et al. Ranibizumab versus verteporfin for neovascular age-related macular degeneration. *N Engl J Med*. 2006;355:1432-1444.
33. Rosenfeld PJ, Brown DM, Heier JS, et al. Ranibizumab for neovascular age-related macular degeneration. *N Engl J Med*. 2006;355:1419-1431.
34. Saint-Geniez M, Kurihara T, Sekiyama E, Maldonado AE, D'Amore PA. An essential role for RPE-derived soluble VEGF in the maintenance of the choriocapillaris. *Proc Natl Acad Sci USA*. 2009;106:18751-18756.
35. Tranos P, Vacalis A, Asteriadis S, et al. Resistance to antivascular endothelial growth factor treatment in age-related macular degeneration. *Drug Des Devel Ther*. 2013;7:485-490.
36. Illendula A, Gilmour J, Grembecka J, et al. Small molecule inhibitor of CBFβ-RUNX binding for RUNX transcription factor driven cancers. *EBioMedicine*. 2016;8:117-131.
37. Simo R, Carrasco E, Garcia-Ramirez M, Hernandez C. Angiogenic and antiangiogenic factors in proliferative diabetic retinopathy. *Curr Diabetes Rev*. 2006;2:71-98.
38. Madge LA, Pober JS. TNF signaling in vascular endothelial cells. *Exp Mol Pathol*. 2001;70:317-325.
39. Pober JS. Endothelial activation: intracellular signaling pathways. *Arthritis Res*. 2004;4(Suppl 3):S109-S116.
40. Zhou P, Lu S, Luo Y, et al. Attenuation of TNF-α-induced inflammatory injury in endothelial cells by Ginsenoside Rb1 via inhibiting NF-κB, JNK and p38 Signaling Pathways. *Front Pharmacol*. 2017;8:464.
41. Jayakumar AR, Taherian M, Panickar KS, et al. Differential response of neural cells to trauma-induced swelling in vitro. *Neurochem Res*. 2018;43:397-406.
42. Watanabe H, Ishibashi K, Mano H, et al. Mutant p53-expressing cells undergo necroptosis via cell competition with the neighboring normal epithelial cells. *Cell Rep*. 2018;23:3721-3729.
43. Fan Y, Xue W, Schachner M, Zhao W. Honokiol eliminates glioma/glioblastoma stem cell-like cells via JAK-STAT3 signaling and inhibits tumor progression by targeting epidermal growth factor receptor. *Cancers*. 2018;11:22.
44. Khalilpourfarshbafi M, Devi Murugan D, Abdul Sattar MZ, Sucedaram Y, Abdullah NA. Withaferin A inhibits adipogenesis in 3T3-F442A cell line, improves insulin sensitivity and promotes weight loss in high fat diet-induced obese mice. *PLoS One*. 2019;14:e0218792.
45. Ennis BW, Fultz KE, Smith KA, et al. Inhibition of tumor growth, angiogenesis, and tumor cell proliferation by a small molecule inhibitor of c-Jun N-terminal kinase. *J Pharmacol Exp Ther*. 2005;313:325-332.
46. Souvannaseng L, Hun LV, Baker H, et al. Inhibition of JNK signaling in the Asian malaria vector Anopheles stephensi extends mosquito longevity and improves resistance to Plasmodium falciparum infection. *PLoS Pathog*. 2018;14:1-39.
47. Xiao GY, Mohanakrishnan A, Schmid SL. Role for ERK1/2-dependent activation of FCHSD2 in cancer cell-selective regulation of clathrin-mediated endocytosis. *PNAS*. 2018;115:e9570-e9579.
48. Reinhard C, Shamoon B, Shyamala V, Williams LT. Tumor necrosis factor alpha-induced activation of c-jun N-terminal kinase is mediated by TRAF2. *EMBO J*. 1997;16:1080-1092.
49. Gupta K, Kshirsagar S, Li W, et al. VEGF prevents apoptosis of human microvascular endothelial cells via opposing

effects on MAPK/ERK and SAPK/JNK signaling. *Exp Cell Res*. 1999;247:495-504.

50. Papachristou DJ, Batistatou A, Sykiotis GP, Varakis I, Papavassiliou AG. Activation of the JNK-AP-1 signal transduction pathway is associated with pathogenesis and progression of human osteosarcomas. *Bone*. 2003;32:364-371.
51. Elsasser A, Franzen M, Kohlmann A, et al. The fusion protein AML1-ETO in acute myeloid leukemia with translocation t(8;21) induces c-jun protein expression via the proximal AP-1 site of the c-jun promoter in an indirect, JNK-dependent manner. *Oncogene*. 2003;22:5646-5657.
52. Martinez M, Hinojosa M, Trombly D, et al. Transcriptional auto-regulation of RUNX1 P1 promoter. *PlosOne*. 2016;11 :e0149119.
53. Deng Y, Ren X, Yang L, Lin Y, Wu X. A JNK-dependent pathway is required for TNFα-induced apoptosis. *Cell*. 2003;115:61-70.
54. Zhang B, Wu T, Wang Z, et al. p38MAPK activation mediates tumor necrosis factor-α-induced apoptosis in glioma cells. *Mol Med Rep*. 2014;11:3101-3107.
55. Stadheim TA, Kucera GL. c-Jun N-terminal kinase/stress-activated protein kinase (JNK/SAPK) is required for mitoxantrone- and anisomycin-induced apoptosis in HL-60 cells. *Leuk Res*. 2002;26:55-65.
56. Byrne AM, Bouchier-Hayes DJ, Harmey JH. Angiogenic and cell survival functions of vascular endothelial growth factor (VEGF). *J Cell Mol Med*. 2005;9:777-794.
57. Brusselmans K, Bono F, Collen D, Herbert J-M, Carmeliet P, Dewerchin M. A novel role for vascular endothelial growth factor as an autocrine survival factor for embryonic stem cells during hypoxia. *J Biol Chem*. 2005;280:3493-3499.
58. Morita K, Suzuki K, Maeda S, et al. Genetic regulation of the RUNX transcription factor family has antitumor effects. *J Clin Invest*. 2017;127:2815-2828.
59. Reiter CEN, Gardner TW. Functions of insulin and insulin receptor signaling in retina: possible implications for diabetic retinopathy. *Prog Retina Eye Res*. 2003;22:545-562.
60. Bressler SB, Beaulieu WT, Glassman AR, et al. Factors associated with worsening proliferative diabetic retinopathy in eyes treated with panretinal photocoagulation or Ranibizumab. *Ophthalmol*. 2017;124:431-439.
61. Zhao Y, Singh RP. The role of anti-vascular endothelial growth factor (anti-VEGF) in the management of proliferative diabetic retinopathy. *Drugs Context*. 2018;7:e212532.
62. Ye N, Ding Y, Wild C, Shen Q, Zhou J. Small molecule inhibitors targeting Activator Protein 1 (AP-1). *J Med Chem*. 2014;57:6930-6948.

SUPPORTING INFORMATION

Additional supporting information may be found online in the Supporting Information section.

How to cite this article: Whitmore HAB, Amarnani D, O'Hare M, et al. TNF-α signaling regulates RUNX1 function in endothelial cells. *The FASEB Journal*. 2021;35:e21155. https://doi.org/10.1096/fj.202001668R